Available online at www.sciencedirect.com
SCIENCE DIRECT
Genomics 87 (2006) 616–632
GENOMICS
www.elsevier.com/locate/ygeno

Overlapping and distinct transcriptional regulator properties of the GLI1 and GLI2 oncogenes

Thomas Eichberger [1], Veronika Sander [1], Harald Schnidar, Gerhard Regl, Maria Kasper, Carmen Schmid, Sandra Plamberger, Alexandra Kaser, Fritz Aberger, Anna-Maria Frischauf *

Department of Molecular Biology, University of Salzburg, Hellbrunnerstrasse 34, A-5020 Salzburg, Austria

Received 22 September 2005; accepted 8 December 2005
Available online 24 January 2006

Abstract

The GLI transcription factors mediate the hedgehog signal in development and carcinogenesis. Basal cell carcinoma can be caused by overexpression of either GLI1 or GLI2. Though GLI1 and GLI2 have identical or very similar DNA binding specificities, some of their activities are overlapping, some are clearly distinct. We analyzed target gene specificities of GLI1 and constitutively active GLI2 (GLI2ΔN) by global expression profiling in an inducible, well-characterized HaCaT keratinocyte expression system. Four hundred fifty-six genes up- or downregulated at least twofold were identified. GLI target gene profiles correlated well with the biological activities of these transcription factors in hair follicles and basal cell carcinoma. Upregulation of largely overlapping sets of target genes was effected by both factors, repression occurred predominantly in response to GLI2. Also, significant quantitative differences in response to GLI1 and GLI2ΔN were found for a small number of activated genes. Since we have not detected a putative processed GLI2 repressor, these results point to specific but indirect target gene repression by GLI2ΔN via preferential activation of one or more negative regulators.

Keywords: Basal cell carcinoma; GLI target genes; Global expression analysis; Keratinocytes; Transcriptional repression

The hedgehog (Hh) signaling pathway (reviewed in [1,2]) has been implicated not only in development, but also in the formation and maintenance of different tumors of skin, brain, prostate, upper gastrointestinal tract, and lung (reviewed in [3–8]). The tumorigenic effect of constitutive hedgehog signaling was first demonstrated in basal cell carcinoma (BCC), in which the majority of tumors are caused by the inactivation of the Hh receptor and negative pathway regulator PTCH [9–11]. In addition, mutations in SMOH leading to constitutive pathway activation have been found in sporadic BCC [12,13]. Pathway activation by overexpression of Sonic hedgehog (SHH) in human keratinocytes or mouse skin also leads to BCC-like features and changes in gene expression [14,15]. The zinc finger transcription factors GLI1 and GLI2, the main mediators of the hedgehog signal in skin, can both cause epithelial tumors with characteristics of BCC when overexpressed in the basal epidermal layer and the outer root sheath of the hair follicle in transgenic mice and frog skin [16–20]. Overlapping function between GLI1 and GLI2 in development, however, is apparent from the different phenotypes of single and compound mutants [21–27] and has most clearly been demonstrated by the rescue of the *Gli2*$^{-/-}$ developmental phenotype in mice expressing *Gli1* from the *Gli2* locus, except for a subtle, unexplained skin phenotype [28]. GLI1 and GLI2 have been shown to have distinct as well as overlapping functions. Though GLI1 has been shown to have activator functions only [29–32], GLI2 can clearly act as an activator as proven by the substitution experiment referred to above, but there is also evidence for repressive function of GLI2 [24,30,32–34]. Differences in the biological activities of Gli1 and Gli2 exist, since *Gli1*$^{-/-}$ mice have no obvious phenotype, while homozygous *Gli2*$^{-/-}$ mice die around birth and have abnormal lungs and neural tube and also defects in hair follicle development [21,27,35,36].

Data on the respective roles of GLI1 and GLI2 in tumorigenesis are less extensive. Using a conditional *Gli2* allele Hutchin et al. [37] showed that BCC-like tumor growth

* Corresponding author. Fax: +43 662 8044 183.
E-mail address: annemarie.frischauf@sbg.ac.at (A.-M. Frischauf).
[1] These authors contributed equally to this work.

0888-7543/$ - see front matter © 2005 Elsevier Inc. All rights reserved.
doi:10.1016/j.ygeno.2005.12.003

and maintenance depend on continuous expression of *Gli2* in tumor cells. GLI1 is the hedgehog target gene most consistently expressed at elevated levels in BCC and in the majority—if not all—Hh-associated tumors [16,38,39]. GLI1 has been shown to be important in growth and maintenance of prostate tumor cells [38,40]. GLI1 is also likely to play a critical role in medulloblastoma, where it is highly expressed. In *Gli1*$^{-/-}$ mice the incidence of medulloblastoma caused by constitutive Hh signaling [41] is severely reduced even though it can occur. Less is known about the role of GLI2 in Hh signaling-induced tumors.

To define the relative contributions of these transcription factors to carcinogenesis, we focused on basal cell carcinoma, where the action of GLI1 or GLI2 is sufficient to give rise to tumors. To assess on a molecular level the extent of overlapping and distinct target gene specificities of GLI1 and GLI2, we used conditional expression in the human keratinocyte cell line HaCaT [42], in whic h we have previously shown that (i) the response to GLI1 and GLI2 is similar to that of primary human keratinocytes and (ii) GLI1 and GLI2 can elicit expression patterns that resemble to a significant extent those of BCC [43]. Here, we have addressed by global expression profiling and QRT-PCR the target gene specificities of the transcriptional activators GLI1 and GLI2ΔN, a constitutively active form of GLI2 lacking the N-terminal repression domain [44]. Human full-length GLI2 was recently described by Roessler and colleagues [34] and shows significantly lower transcriptional activator function than GLI2ΔN in vitro. In vivo, in mouse hair follicle development, there is evidence that full activation of Gli2 depends on an event that requires the presence of Shh. In the absence of Shh, rescue of the phenotype can be achieved only by a constitutively active, N-terminally truncated Gli2 protein that closely resembles the human GLI2ΔN [36]. Similarly, only truncated/activated Gli2 is able to mimic Shh-induced gene expression in isolated presomitic mesoderm [24,30]. N-terminally truncated Gli2 has also been shown to produce a more severe tumor phenotype than full-length Gli2 when expressed in the epidermis of transgenic mice [19]. The truncated human GLI2, GLI2ΔN, is therefore a valuable tool to mimic the activated form of GLI2. When we used DNA-array technology to analyze the transcription profiles induced by conditionally expressed GLI2ΔN and GLI1, we identified qualitative and quantitative similarities as well as differences in their target gene response. Only very few genes were upregulated exclusively by either GLI1 or GLI2ΔN. The most striking difference between GLI1 and GLI2ΔN was the very small number of genes repressed on induction of GLI1, while a large number were repressed after induction of GLI2ΔN. In the absence of evidence for proteolytic processing and in view of the strongly activating properties of GLI2ΔN, repression of target genes in this system is likely to be indirect, possibly by GLI2 specific activation of a repressor. The data provide evidence for selective activation of transcriptional programs by GLI1 and GLI2, which could have significant consequences for the execution of the hedgehog signal in keratinocytes.

Results and discussion

Differential induction and repression of GLI1 and GLI2 target genes

To compare GLI1 and GLI2 expression profiles in keratinocytes we used tetracycline-inducible HaCaT cell lines expressing GLI1 or an activated form of GLI2 (GLI2ΔN) [43]. To minimize cell clone-specific effects we pooled four independent clones. Since a comparison of the relative effects of GLI1 and GLI2ΔN has to be based on similar expression levels of the transcription factors, we first measured transgene expression by QRT-PCR at the RNA level. Both GLI1 and GLI2ΔN were expressed at comparable levels in the induced cells used for the expression analysis (Fig. 1A). Fig. 1A shows that the increase in PTCH mRNA reflects the increase in GLI1 and GLI2ΔN mRNA levels, implying similar transcriptional activity of both GLI proteins. We also demonstrated induction of GLI1 and GLI2ΔN by Western blot (Fig. 1A, top). To compare activity and specificity of GLI1, GLI2ΔN, and the newly described full-length GLI2 [34], we used luciferase assays on three different promoters: the known target genes PTCH [45] (C. Schmid, unpublished) and GLI1 [46] and an artificial promoter containing six tandem GLI binding sites [47] (Fig. 1B). Activation of all three promoters is strongest with GLI2ΔN, followed by GLI1 and full-length GLI2. The relative activities of the three GLI proteins, however, vary widely on the three tested promoters. Differential activity of different GLI proteins on different promoters is frequently observed and may be partly responsible for different effects of the transcription factors as discussed below.

Approximately 12,000 PCR-amplified, sequence-verified EST clones on high-density filter arrays were hybridized with ^{33}P-labeled cDNA from GLI1- or GLI2ΔN-expressing and control cells to determine expression levels after 24 and 72 h of tetracycline treatment (see Material and methods). In total, RNA levels of 456 genes represented by 512 EST clones were found to be increased or decreased at least twofold at one or both time points as judged by SAM (significance analysis of microarray) [48] (Table 1). Fig. 2 compares the inducing and repressing activities of GLI1 and GLI2ΔN. Seventy-two hours after induction 68 genes were induced more than twofold by GLI1 and 138 by GLI2ΔN, 46 of these were induced by both. Most genes upregulated by GLI2ΔN were also upregulated by GLI1. The smaller number of genes responding to GLI1 than GLI2ΔN may reflect the fact that for many genes the strength of the response was higher for GLI2ΔN than for GLI1. For a very small number of genes there is such a large difference between the activation by the two transcription factors that expression of those genes can be considered specific to just GLI1 or GLI2. For GLI2 induction of BCL2 such specificity has previously been described [49]. Here we find GLI2 specificity also for FST, while TNC and CTSL are much more strongly activated by GLI1 than by GLI2ΔN (Table 1 and Fig. 5). It is possible that a gene-specific threshold of GLI activity is required, but the detailed mechanism is not known.

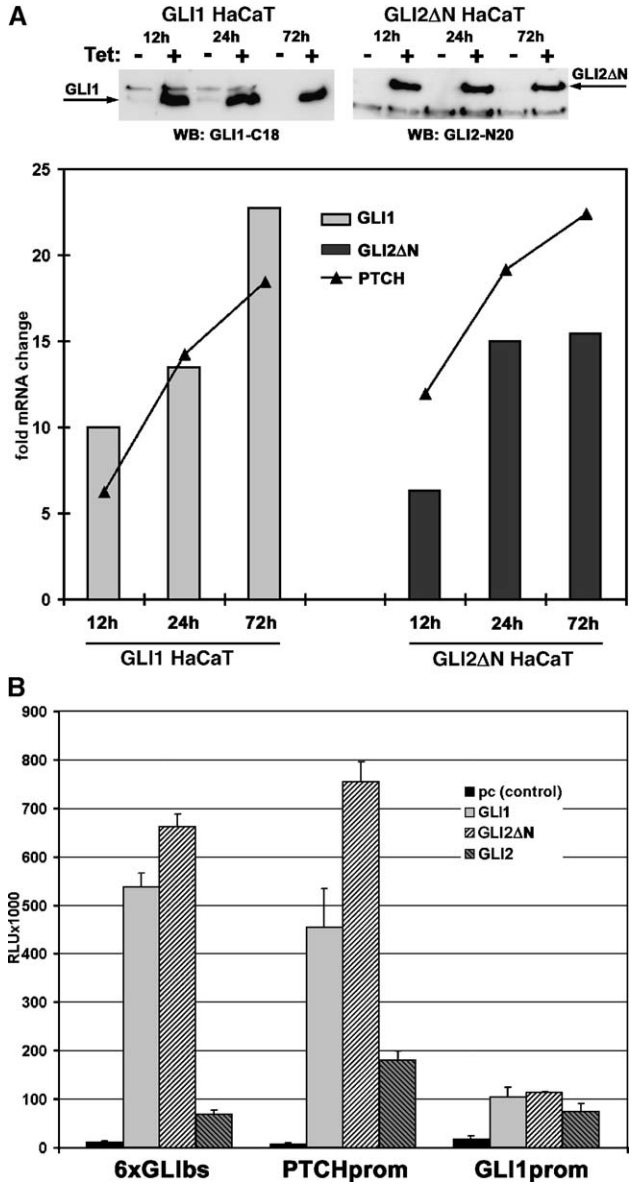

Fig. 1. Transcriptional activity of GLI1 or GLI2ΔN in HaCaT keratinocytes. (A) The induction in HaCaT cells of GLI1 and GLI2ΔN under tetracycline control was determined by QRT-PCR and Western blot. Increase of the GLI1 or GLI2ΔN transgene and the direct target gene PTCH mRNAs is shown after induction for the times indicated. GLI1 and GLI2ΔN proteins (top) were detected using specific antibodies against GLI1 and GLI2. Samples were taken from tetracycline-treated and untreated double stable HaCaT cells as indicated. (B) Luciferase reporter assay comparing the activities of GLI1, GLI2ΔN, and human full-length GLI2 on different promoter constructs. HaCaT cells were cotransfected with different reporter constructs (the synthetic reporter construct 6×GLIbs, PTCHprom, and GLI1prom) and NLS-Myc-tagged GLI1 (GLI1), Myc-tagged GLI2ΔN (GLI2ΔN), Myc-tagged full-length GLI2 (GLI2), or empty expression vector (pc).

Reduction of expression levels was observed for only 45 clones after 72 h of tetracycline treatment by GLI1 compared to 190 genes for GLI2ΔN; 28 of these were repressed by both. The results are even more striking at the 24-h time point, at which twice as many genes were induced, but 17 times as many repressed by GLI2ΔN compared to GLI1. A large majority of genes repressed by GLI2ΔN are not affected by GLI1, while only a very small number of genes repressed in response to GLI1 are unaffected by GLI2ΔN expression. Most genes repressed by GLI1 are also repressed by GLI2ΔN. Since in GLI1-expressing HaCaT cells endogenous GLI2 is also turned on after a delay [43], it is not possible to discriminate between a specific effect of GLI1 and an indirect effect via GLI1-induced expression of endogenous GLI2. These results show a clear difference between the regulatory effects of GLI1 and GLI2ΔN in keratinocytes compatible with in vivo data in other systems showing only activating function for Gli1, but activating and repressing function for Gli2 [24,30,32–34]. It is surprising that repression can take place in the absence of the putative N-terminal repressor domain of GLI2 [30,34]. The data, however, do not address whether repression of target genes is caused directly by a GLI2 repressor function present also in GLI2ΔN or indirectly by GLI2-mediated induction of an unknown repressor activity. Ci, the single *Drosophila* ortholog of the three mammalian GLI transcription factors, can act either as activator or as repressor of transcription. In the presence of Hh, an activated form of full-length 155-kDa Ci induces the expression of *Hh* target genes, while in the absence of Hh a proteolytically processed 75-kDa repressor form is localized to the nucleus and prevents the expression of *Hh* target genes (reviewed in [1,2]). Of the three mammalian GLI proteins [50], mouse Gli1 has been described as having only activating functions, which can be supplied also by mouse Gli2 [21,28]. Mouse Gli3 is an important repressor of *Hh* target genes in limb and neural development [51,52], but also has an activating function [24,53]. In vitro, all three GLI proteins have been shown to be able to act as dominant negative, if the protein is truncated C-terminally to the Zn-finger DNA binding domain [23,30,32,54], indicating the presence of activating domains in the deleted fragment. The structure of these molecules is similar to that of the in vivo-processed 75-kDa repressor form of Ci [23,32].

The repressor activity of C-terminally truncated Gli3 has been amply demonstrated in vivo and in vitro [23,51,54,55]. The in vivo repressor role of a corresponding truncated Gli2 protein is much less clear. Unlike Gli3, the repressing activity of Gli2 observed in some contexts is not responsive to the Hh signal. Truncated products of Gli2 have been observed after expression in frog embryos [23], COS cells [51], and *Drosophila melanogaster* [32], but there is no clear evidence for such a repressor form in the absence of ectopic overexpression.

Phosphorylation by protein kinase A (PKA) is a precondition for proteolytic processing of Ci and of Gli3 to a C-terminally truncated form with repressor activity [23,56–58]. In the expression analysis the large number of genes repressed in response to GLI2ΔN could arise due to either direct repression by a modified form of GLI2ΔN or another mechanism. We therefore first assayed for forskolin-induced PKA phosphorylation of the GLI proteins by immunoprecipitation using GLI1- and GLI2ΔN-specific antibodies followed by detection using PKA substrate-specific antibody (Fig. 3A). We then looked for the appearance of proteolytically processed forms of the GLI proteins in Western blots of whole lysates

from cells treated with tetracycline and forskolin, but only full-length specific fragments were detected (Fig. 3B). We therefore conclude that detectable processing of the inducible GLI2ΔN protein in a way comparable to that of Ci or GLI3 does not occur in HaCaT cells even though strong repression of target genes is observed.

Groups of functionally related genes regulated by GLI1 and GLI2

Based on their molecular function and association with pathways, we grouped the differentially expressed genes according to gene map classification using Pathway Explorer (https://www.pathwayexplorer.genome.tugraz.at/) [59] (Fig. 4 and Table 1). As expected, cell cycle and proliferation are among the most highly represented classes. Two pathways known to interact with HH, WNT and TGFβ, also appear. These and other classes are discussed below in the context of skin, BCC, and hair follicles.

To verify a subset of the array data we used QRT-PCR (genes marked by superscript "b" in Table 1). For selected genes we refined the time resolution by a 12-h point (Fig. 5 and Table 2). The QRT-PCR data show good agreement with the array data for kinetics and level of induction. The higher fold-change values measured by QRT-PCR are a common phenomenon, likely to be due to the higher dynamic range of the PCR-based approach.

We have previously shown that GLI2ΔN induces the expression of genes driving proliferation and represses epidermal differentiation markers [60]. We now compared these results to the GLI1 response and observed very little repression of differentiation markers such as KRT1, KRT10, IVL, SPRR2A (Table 2, bottom), DSG1, S100A8, and S100A9 (Table 1), while genes involved in promoting proliferation were induced also by GLI1 (Table 2, top), illustrating the distinct and overlapping specificities of the effects of the two related transcription factors. Cell cycle genes regulated by GLI1 and GLI2ΔN include some cyclins, cyclin inhibitors, cyclin-dependent kinases, and other proteins involved in critical steps of cell cycle progression such as E2F1. Increased cell cycle progression is also seen in the mRNA increase of the classical markers MKI67 (Ki67), PCNA, and MAD2L1 (Table 1), a mitotic checkpoint protein induced by E2F1 [61].

Differential expression in response to GLI1 or GLI2ΔN was also found for different proteases and their inhibitors, though this does not necessarily correlate with their activity since protease activity is mostly regulated at the posttranslational level. Of the members of the kallikrein family of serine proteases expressed in skin, KLK6 was highly and KLK5 and KLK10 were moderately induced by both GLI1 and GLI2ΔN (Fig. 5A). The serine protease inhibitor Kazal-type 5 (SPINK5) (Table 1), which is coexpressed with kallikrein proteases in skin, is downregulated by GLI2ΔN only. Expression of several other serine protease inhibitors is also changed by GLI expression: SERPINA1 and SERPINB2 are upregulated, while SERPINB3, SERPINB5, and SERPINB13 are turned down, as is the epithelial-specific protease inhibitor PI3 (SKALP/elafin) (Fig. 5D and Table 1). An example of the complementary regulatory roles of GLI1 and GLI2ΔN is the lysosomal cysteine protease cathepsin L (CTSL), which is also expressed in skin and hair follicles. CTSL is upregulated in response to GLI1 and to a lower extent by GLI2ΔN, while its inhibitor cystatin A (CSTA) is downregulated by GLI2ΔN only (Figs. 5B and 5D). The metalloproteases illustrate opposite effects in successive regulatory steps: MMP1, MMP10, MMP12, and MMP13 show a strong negative response to GLI2ΔN and a weaker one to GLI1 expression (Table 1). From the higher time resolution of the QRT-PCR analysis for MMP1, MMP10, and MMP13 it is clear that repression is reversed at the 72-h time point (Fig. 5D, inset). This is likely to be mediated by the transcription factor FOXE1, a direct target gene of GLI2 [62], which strongly induces expression of these MMPs when expressed in HaCaT keratinocytes (data not shown).

GLI2ΔN plays an essential role in hair follicle development [36] and is highly expressed in the outer root sheath (ORS) [46]. We found significant similarities between genes expressed in hair follicles and HaCaT cells expressing GLI2ΔN. BCCs are another structure expressing GLI target genes. Some genes expressed in the ORS and in BCCs are upregulated by GLI2ΔN in HaCaT cells (CTSL, FOXE1, BCL2) (Fig. 5C), while most of the downregulated genes (KRT1, KRT10, IVL, DSG1) (Fig. 5D and Table 1) are not normally present in the basal layer of epidermis, the ORS, and BCCs. The protease CTSL (see above) has also been localized to the ORS. Its importance in proper skin and hair morphology is underlined by the phenotype of CTSL-deficient mice, which develop epidermal hyperplasia, acanthosis, hyperkeratosis, and periodic hair loss [63–65]. CTSL is also elevated in BCC [66]. An important role in development and cycling of the hair follicle and skin homeostasis involves TGFβ signaling. Members of the TGFβ family are involved in the control of keratinocyte proliferation and differentiation during normal skin stratification (reviewed in [67–69]). We found upregulation of expression of the activin/BMP antagonists follistatin (FST) and HTRA1 (PRSS11) (Fig. 5C and Table 1), pointing to inhibition of TGFβ signaling by the HH/GLI pathway. Notably, FST was specifically induced by GLI2, while HTRA1 responded to both GLI1 and GLI2ΔN. This correlates well with the expression of follistatin mRNA in mouse skin in the ORS of the hair follicle and in the basal layer of the epidermis [70]. In follistatin-deficient mice, hair follicle development is significantly retarded, while the number of hair follicles in wild-type embryonic skin explants treated with follistatin is increased [71]. Furthermore, the activators of TGFβ signaling, BMP2 and BMP7, were downregulated by GLI2, as was their target gene *ID1* (Table 1) [72–74], a basic helix–loop–helix transcription factor involved in mediating the effect of TGFβ. TGFβ receptor2 (*TGFBR2*) is also downregulated. Together, these results point to an inhibitory role of GLI2 on TGFβ signaling in hair follicle development.

Conclusions

Target gene expression after induction of GLI1 and GLI2 in HaCaT keratinocytes illustrates the proliferation enhancing

Table 1
Gene expression profiles of human epidermal cells in response to GLI1 and GLI2ΔN

HUGO gene name	NCBI acc. no.	Fold induction/repression				Pathway ID
		GLI1 24 h	GLI1 72 h	GLI2 24 h	GLI2 72 h	
SERPINB3[a,b]	NM_006919	**0.38**	**0.39**	**0.03**	**0.02**	1
S100A8[a,b]	NM_002964	**0.35**	**0.24**	**0.09**	**0.02**	10
KRT1[a,b]	NM_006121	0.64	–	**0.12**	**0.02**	
JUNB[a,b]	NM_002229	–	**0.38**	–	**0.05**	26, 29
KRT10[a,b]	NM_000421	0.61	**0.50**	**0.14**	**0.06**	
CBLNL4	NM_080617	**0.43**	**0.44**	**0.15**	**0.06**	
PI3[a,b]	NM_002638	**0.30**	**0.26**	**0.22**	**0.06**	1, 25
ABCA4[a,b]	NM_000350	**0.49**	0.61	**0.17**	**0.08**	
FLJ22709[a]	NM_024578	–	–	**0.17**	**0.09**	
MMP13[a,b]	NM_002427	**0.45**	0.52	**0.07**	**0.10**	4, 25
THBD[a]	NM_000361	–	0.58	**0.26**	**0.12**	
MMP1[a,b]	NM_002421	**0.46**	0.65	**0.39**	**0.12**	4, 25
SPRR2A[a,b]	NM_005988	**0.40**	**0.37**	**0.21**	**0.13**	
S100A9[a,b]	NM_002965	–	**0.27**	**0.40**	**0.13**	10
CLCA4	NM_012128	**0.42**	**0.28**	**0.22**	**0.14**	23
CLECSF2	NM_005127	–	–	**0.26**	**0.14**	11
PLA2G2A[a]	NM_000300	–	**0.23**	**0.35**	**0.14**	41
VAV3[a]	NM_006113	–	–	**0.27**	**0.15**	3, 5
CCL2[a]	NM_002982	–	–	–	**0.15**	2, 10, 11, 19
GJA1[a]	NM_000165	–	1.85	**0.16**	**0.17**	28, 38
CSTA[a,b]	NM_005213	–	–	**0.18**	**0.17**	1
LINCR	AL389981	0.60	**0.49**	**0.32**	**0.18**	
ID1[a,b]	NM_002165	–	**0.50**	**0.41**	**0.18**	
OLFM4[a]	NM_006418	**2.28**	0.65	**0.44**	**0.19**	
BIC transcript	AF402776	–	0.52	**0.49**	**0.20**	
KRT23	NM_015515	0.58	**0.29**	0.57	**0.20**	
NCF2[a]	NM_000433	–	**0.47**	**0.23**	**0.21**	27
HPGD[a]	NM_000860	0.52	**0.48**	**0.13**	**0.22**	22
BCKDK[a]	NM_005881	–	–	**0.19**	**0.22**	
CA2[a]	NM_003716	–	–	**0.23**	**0.22**	27
GPR174[a]	NM_032553	–	0.59	**0.39**	**0.22**	7
GPNMB	NM_001005340	–	–	**0.38**	**0.23**	
MPPED2	NM_001584	–	0.65	**0.39**	**0.23**	
ADM[a]	NM_001124	–	–	**0.39**	**0.23**	15, 38
GJB6	NM_006783	–	–	**0.41**	**0.23**	28, 39
ZIC2[a]	NM_007129	0.53	**0.45**	**0.42**	**0.23**	
VAX2	NM_012476	–	–	0.54	**0.23**	
MMP10[a,b]	NM_002425	0.58	**0.46**	**0.24**	**0.24**	4, 25
UGCGL1[a]	NM_001025777	0.52	0.58	**0.27**	**0.25**	
SCAMP1	NM_004866	–	–	**0.33**	**0.25**	
OVOL2[a]	NM_021220	–	0.55	0.56	**0.25**	
MYC[a,b]	NM_002467	–	**0.45**	**0.42**	**0.26**	8, 31, 33, 35
KRT4[a]	NM_002272	0.53	**0.39**	**0.45**	**0.26**	
NID[a]	NM_002508	–	–	**0.38**	**0.27**	25
FAT2[a]	NM_001447	–	0.58	**0.43**	**0.27**	
PRKACA	NM_002730	–	–	**0.43**	**0.27**	37, 38, 39
RHOH[a]	NM_004310	–	–	**0.39**	**0.28**	
S100A12	NM_005621	–	–	0.66	**0.28**	10, 27
SHANK2	NM_133266	–	–	**0.32**	**0.29**	
CEACAM6[a]	NM_002483	–	**0.43**	**0.42**	**0.29**	
None	CAA6762	–	–	0.55	**0.29**	
EPHA4	NM_004438	–	0.60	–	**0.29**	
SERPINB5[a,b]	NM_002639	–	–	**0.28**	**0.30**	1, 14
PTPRZ1[a]	NM_002851	–	–	**0.31**	**0.30**	
CLDN8[a]	NM_199328	0.58	**0.43**	**0.38**	**0.30**	28
SBF2	NM_030962	–	–	**0.41**	**0.30**	
RASSF6	NM_177532	–	0.57	**0.44**	**0.30**	
PRNP[a]	NM_000311	–	–	**0.48**	**0.30**	
GJB2[a]	NM_004004	–	–	**0.50**	**0.30**	28, 39
IFNGR1[a]	NM_000416	–	–	**0.34**	**0.31**	

Table 1 (*continued*)

HUGO gene name	NCBI acc. no.	Fold induction/repression				Pathway ID
		GLI1 24 h	GLI1 72 h	GLI2 24 h	GLI2 72 h	
IKBKE[a]	NM_014002	–	–	**0.48**	**0.31**	
None[a]	AP001695	–	–	**0.48**	**0.31**	
HIST1H2AM	NM_003514	–	0.59	–	**0.31**	16, 20, 24, 29
ITGA6[a]	NM_000210	–	–	**0.29**	**0.32**	
DST	NM_001723	–	–	**0.46**	**0.32**	
TMEM45A[a]	NM_018004	–	–	**0.42**	**0.33**	
CSRP2[a]	NM_001321	–	–	**0.32**	**0.34**	8, 17
DSG1[a]	NM_001942	–	–	**0.32**	**0.34**	28
ATP1B3P1[a]	AF005898	–	–	**0.38**	**0.34**	
ALDH3A1[a]	NM_000691	–	–	**0.50**	**0.34**	27
ACE2	NM_021804	–	–	–	**0.34**	
MAF[a]	NM_001031804	–	–	**0.31**	**0.35**	26, 29
ENSG00000146394[a]	AF116669	–	–	**0.34**	**0.35**	
ZNF230[a]	NM_006300	–	–	**0.34**	**0.35**	
SAMD9[a]	NM_017654	–	0.66	**0.41**	**0.35**	
DLX1[a]	NM_178120	–	–	**0.41**	**0.35**	
ATP1B3[a]	NM_001679	–	–	**0.48**	**0.35**	39
AKAP4[a]	NM_003886	–	0.60	**0.49**	**0.35**	14, 37
VARS2L	NM_020442	–	–	**0.49**	**0.35**	18
HOXA9[a]	NM_002142	–	–	0.51	**0.35**	
MAPK6[a]	NM_002748	–	–	–	**0.35**	37
NPL	NM_030769	–	–	–	**0.35**	
HEY1[a,b]	NM_001002953	–	–	**0.38**	**0.36**	
PLAU[a]	NM_002658	0.62	**0.47**	**0.43**	**0.36**	
VDR[a]	NM_002658	–	–	**0.43**	**0.36**	19, 33, 40
LUM[a]	NM_002345	–	–	**0.44**	**0.36**	25
AIM1	NM_001624	–	–	–	**0.36**	
ABCA1[a]	NM_005502	–	–	**0.37**	**0.37**	21, 41
SNCG	NM_003087	–	**0.46**	**0.43**	**0.37**	
PYGL	NM_002863	–	–	**0.43**	**0.37**	
TMOD3	NM_014547	–	–	0.51	**0.37**	6
MALAT1[a]	AF203815	–	–	0.51	**0.37**	
RAP1GA1	NM_002885	–	–	0.64	**0.37**	3, 27
DEFB1[a]	NM_005218	–	0.63	–	**0.37**	
TGFBR2	NM_001024847	–	–	–	**0.37**	34
LTB4R2	NM_019839	–	–	0.55	**0.38**	7, 13
ALDH6A1	NM_005589	–	**0.38**	0.56	**0.38**	
SPINK5	NM_006846	–	–	0.58	**0.38**	1, 11
TIMP3	NM_000362	–	–	0.62	**0.38**	1, 4, 25
HCCS	NM_005333	–	**0.50**	0.64	**0.38**	
CDKN2B	NM_004936	–	–	–	**0.38**	1, 31
CNTN1	NM_001843	–	–	–	**0.38**	
C6orf51	NM_138408	–	–	**0.45**	**0.39**	
PERP[a]	NM_022121	–	–	0.56	**0.39**	
TncRNA[a]	AF001892	–	–	0.58	**0.39**	
AKR1C4	NM_001818	–	–	–	**0.39**	23
KIAA1815	NM_024896	–	–	–	**0.39**	
CDKN1A[a,b]	NM_000389	0.60	0.60	**0.29**	**0.40**	1, 31
ETFA[a]	NM_000126	–	–	**0.34**	**0.40**	
MCM7[a]	NM_005916	0.60	0.58	**0.39**	**0.40**	26, 29, 31, 32
DLX3[a,b]	NM_005220	–	0.62	0.52	**0.40**	
FZD6	NM_003506	–	–	–	**0.40**	
UBAP2	NM_018449	–	–	–	**0.40**	
FBLN5	NM_006329	–	–	–	**0.41**	25
MAP3K8[a]	NM_005204	–	–	–	**0.41**	27
RAB38[a]	NM_022337	–	–	**0.31**	**0.42**	
KIAA1404	NM_021035	–	0.59	**0.47**	**0.42**	
MAOA[a]	NM_000240	–	–	**0.50**	**0.42**	41
TncRNA	AF001892	–	–	0.52	**0.42**	
ALG8	NM_001007027	–	–	0.52	**0.42**	

(continued on next page)

Table 1 (*continued*)

HUGO gene name	NCBI acc. no.	Fold induction/repression				Pathway ID
		GLI1 24 h	GLI1 72 h	GLI2 24 h	GLI2 72 h	
MEIS1	NM_002398	–	–	0.52	**0.42**	
SERPINB13	NM_012397	–	–	0.59	**0.42**	1
CYB5R3	NM_000398	–	0.65	0.63	**0.42**	15
BMP7[a]	NM_001719	–	0.66	–	**0.42**	2
S100A7[a,b]	NM_002963	**3.06**	**2.14**	–	**0.42**	
RNASE3[a]	NM_002935	–	–	–	**0.42**	
PEX13	NM_002618	–	–	**0.46**	**0.43**	
APCDD1	NM_153000	–	0.64	**0.47**	**0.43**	
FUBP1	NM_003902	–	0.64	0.55	**0.43**	
TM7SF3	NM_016551	–	**0.40**	0.63	**0.43**	
HLA-DRA$_a$	NM_019111	–	–	–	**0.43**	
ROBO1[a]	NM_002941	–	–	**0.40**	**0.44**	
SLC24A3	NM_020689	–	–	**0.42**	**0.44**	
LAMB3[a]	NM_000228	0.66	–	**0.50**	**0.44**	25
EPLIN[a]	NM_016357	–	–	0.55	**0.44**	30
CHRNB1	NM_000747	–	0.58	–	**0.44**	
COL17A1	NM_000494	–	–	–	**0.44**	28
GNG13	NM_016541	–	–	–	**0.44**	37, 38, 39
UGT1	NM_000463	–	–	–	**0.44**	
GABRE	NM_004961	–	–	**0.44**	**0.45**	
ZBTB39	NM_014830	–	–	**0.48**	**0.45**	
KRT16	NM_005557	–	–	0.54	**0.45**	8
IF	NM_000204	–	–	0.58	**0.45**	11
KCNK9	NM_016601	–	–	0.62	**0.45**	
DGKA	NM_001345	–	–	0.63	**0.45**	5
DHRS3	NM_004753	–	**0.42**	–	**0.45**	22
HIST2H2BC	AI016731	–	0.54	–	**0.45**	
CD44	NM_000610	–	–	–	**0.45**	
IQGAP2[a]	NM_006633	–	–	–	**0.45**	1, 3, 6, 30, 36
OLR1	NM_002543	–	–	–	**0.45**	
SQLE[a]	NM_003129	–	–	–	**0.45**	15, 41
NAB1[a,b]	NM_005966	–	–	**0.39**	**0.46**	
BMP2	NM_001200	–	–	**0.45**	**0.46**	2
AKR1C1[a]	NM_001353	–	–	0.52	**0.46**	
ABCA9	NM_080283	–	–	–	**0.46**	
F7	NM_000131	–	–	**0.41**	**0.47**	40
MYO1B	NM_012223	–	–	**0.44**	**0.47**	6, 30
MAZ[a]	NM_002383	1.55	0.59	0.59	**0.47**	
None	CAB4649	–	–	0.61	**0.47**	
SPTBN4	NM_020971	–	–	0.66	**0.47**	6, 30
BCAS1	NM_003657	–	0.58	–	**0.47**	15
UGCG[a]	NM_003358	–	0.64	–	**0.47**	6, 25, 28
DST	NM_001723	–	–	–	**0.47**	
None	AP00049	–	–	–	**0.47**	
RORC	NM_001001523	–	–	–	**0.47**	7
MGST2	NM_002413	0.66	0.58	**0.46**	**0.48**	3, 11, 15, 22
MSX2[a]	NM_002449	–	–	**0.47**	**0.48**	
CLSTN3	NM_014718	–	0.66	0.53	**0.48**	
RBMS2	NM_002898	–	–	0.53	**0.48**	18
RICS[a]	NM_014715	–	–	0.54	**0.48**	
AHNAK	NM_001620	–	0.62	0.57	**0.48**	
LRP1[a]	NM_002332	–	0.52	0.61	**0.48**	8, 21, 24, 41
TIA1	AA485255	–	–	–	**0.48**	
ZNF133	NM_003434	–	–	–	**0.48**	
SLC38A2	NM_018976	–	–	0.51	**0.49**	
BMP1	NM_001199	–	–	0.53	**0.49**	2
NET1	NM_005863	–	–	0.57	**0.49**	17
SCN1B	NM_001037	–	–	0.58	**0.49**	
CXCL1	NM_001511	–	–	0.62	**0.49**	2, 3, 8, 10, 19
CRYAB	NM_001885	–	1.6	–	**0.49**	7

Table 1 (*continued*)

HUGO gene name	NCBI acc. no.	Fold induction/repression				Pathway ID
		GLI1 24 h	GLI1 72 h	GLI2 24 h	GLI2 72 h	
CAP350	NM_014810	–	–	–	**0.49**	
CDK2	NM_001798	–	–	–	**0.49**	9, 31, 32
KRT15	NM_002275	–	–	–	**0.49**	
MCP	NM_002389	–	–	–	**0.49**	11
OAS2[a]	NM_001032731	–	–	–	**0.49**	
PCDH7	NM_002589	–	–	–	**0.49**	
PDCD4	NM_014456	–	–	–	**0.49**	
SRD5A1	NM_001047	–	–	**0.41**	**0.50**	
CEBPB[a]	NM_005194	–	–	**0.49**	**0.50**	10, 37, 40
TNFRSF18	NM_004195	–	–	0.59	**0.50**	
TOB1[a]	NM_005749	–	–	**0.41**	0.51	40
GABRR1	NM_002042	–	–	**0.47**	0.53	
TXN[a]	NM_003329	–	–	**0.39**	0.54	8, 14
SMPDL3A	NM_006714	–	–	**0.45**	0.54	
IGFBP6	NM_002178	–	**0.38**	–	0.54	17, 38
GALNT5	NM_014568	–	**0.49**	–	0.54	
ATP1B1	NM_001001787	–	1.72	**0.32**	0.55	
HFE[a]	NM_000410	–	–	**0.40**	0.55	21
S100P[a]	NM_005980	–	**0.19**	**0.46**	0.55	
FOSL2	NM_005253	–	–	**0.49**	0.55	
GALNT3	NM_004482	–	–	**0.49**	0.56	
NMU	NM_006681	–	0.53	**0.32**	0.57	
IL32[a]	NM_001012631	–	0.53	**0.50**	0.57	
FBXW7	NM_001013415	–	–	**0.39**	0.58	
ERCC5	NM_000123	–	–	**0.45**	0.59	
GP1BB	NM_000407	–	–	**0.47**	0.59	9, 12
None	AF312913	–	–	**0.45**	0.61	
SCFD1	NM_016106	–	–	**0.45**	0.61	
KLKB1	NM_000892	–	0.53	**0.47**	0.61	10
SCNN1A	NM_001038	0.60	**0.36**	0.65	0.61	
MAP3K4	NM_005922	–	–	**0.45**	0.62	36
CSNK1A1	NM_001025105	–	–	**0.50**	0.65	
CDA	NM_001785	–	**0.48**	0.63	0.65	
CTSD[a]	NM_001909	–	**0.48**	–	0.65	
ZNF384	NM_133476	–	–	**0.48**	0.66	
CSNK1A1	NM_001025105	–	–	**0.49**	0.66	
RRM1	NM_001033	–	**2.15**	–	1.51	41
RSAFD1	NM_018264	–	**2.34**	–	1.52	
ITGB1[a]	NM_002211	**2.43**	1.89	1.56	1.59	
DEK	NM_003472	1.77	**2.13**	–	1.63	
CYC1	NM_001916	–	–	**2.12**	1.64	
AREG[a]	NM_001657	1.87	**2.13**	–	1.65	2, 8
EML4	NM_019063	–	–	**2.45**	1.66	
RIPK1	NM_003804	1.72	**2.15**	–	1.66	13, 35
SLC1A4	NM_003038	**2.52**	1.81	**2.50**	1.68	23
ARL6IP	NM_015161	–	1.52	**0.46**	1.74	
RASA4	NM_006989	–	–	**2.00**	1.74	3
EB-1	NM_020140	1.85	**2.46**	–	1.81	
MYLK	NM_005965	**2.40**	**2.88**	**2.39**	1.82	
ECT2	NM_018098	–	**2.66**	–	1.84	
TGFBI	NM_000358	**2.05**	**2.90**	–	1.86	8, 25
PSMB9	NM_002800	1.55	**2.17**	1.87	1.89	40
PPP1CB[a]	NM_002709	1.82	**2.62**	–	1.94	9
FXYD3[a,b]	NM_005971	–	–	**3.53**	1.95	23
MPHOSPH1[a]	NM_016195	–	**2.14**	–	1.95	
TEAD1[a]	NM_021961	–	**2.08**	–	**2.01**	
MS4A6A	NM_022349	1.57	–	–	**2.01**	
JUN	NM_002228	–	–	–	**2.01**	26, 33, 34, 35, 38
PITX1	NM_002653	–	–	–	**2.01**	
LMO4	NM_006769	–	–	1.55	**2.02**	
PLD3	NM_001031696	**2.06**	1.83	–	**2.02**	7

(continued on next page)

Table 1 (*continued*)

HUGO gene name	NCBI acc. no.	Fold induction/repression				Pathway ID
		GLI1 24 h	GLI1 72 h	GLI2 24 h	GLI2 72 h	
ELOVL6	NM_024090	–	–	–	**2.02**	
MTHFD2	NM_006636	–	1.91	–	**2.03**	41
LILRB5	NM_006840	–	–	–	**2.03**	12
GTF2IRD1	NM_005685	–	1.61	–	**2.04**	
NANS	NM_018946	1.63	–	–	**2.04**	15
BARD1	NM_000465	1.54	–	–	**2.06**	
FMN	XM_375185	–	–	–	**2.06**	
SEMA3B	NM_001005914	–	–	1.55	**2.07**	
MCM2	NM_004526	–	–	**2.02**	**2.09**	26, 29, 31, 32
EDG2	NM_001401	–	–	–	**2.10**	37, 38
ZNF264	NM_003417	–	1.70	–	**2.11**	
STK6	NM_003600	–	–	–	**2.11**	
TMEM28	NM_015686	–	1.80	–	**2.12**	
MRAS[a]	NM_012219	1.79	**3.20**	–	**2.14**	
CKMT1	NG_005156	–	–	–	**2.14**	
LGALS9[a]	NM_002308	–	–	–	**2.14**	
LRIG2	NM_014813	–	–	–	**2.15**	
TNFRSF11A	NM_003839	–	1.71	–	**2.16**	
CDK3[a]	NM_001258	1.52	–	–	**2.16**	9
APOBEC3A	NM_145699	–	–	–	**2.16**	
SOX2	NM_003106	–	–	–	**2.16**	16, 20
CD9	NM_001769	–	1.68	1.51	**2.17**	
MKI67[a,b]	NM_002417	–	–	1.68	**2.18**	
EMP2[a]	NM_001424	–	–	**2.48**	**2.18**	8
RFC3	NM_002915	–	–	–	**2.18**	3, 26, 32
CKS2	NM_001827	–	1.96	0.61	**2.20**	9
KLK5[a,b]	NM_012427	1.80	–	**3.26**	**2.21**	
CD84	NM_003874	–	1.60	–	**2.21**	
GSTA4	NM_001512	–	**3.09**	–	**2.22**	
MEOX1[a]	NM_004527.2	–	–	–	**2.22**	
VEGF	NM_001024628	1.66	1.82	1.63	**2.23**	
FYN	NM_002037	–	–	**2.15**	**2.23**	
NCBP1	NM_002486	–	1.59	–	**2.24**	24, 37
RPS5L[a]	NG_000903	**2.45**	**3.87**	–	**2.24**	
RFC4	NM_002916	–	1.99	–	**2.26**	26, 32
BIRC5[a]	NM_001012271	–	1.96	–	**2.27**	1, 12, 13
CTNNA3	NM_003798	1.61	**2.36**	–	**2.27**	13
RGS2	NM_002923	1.56	–	–	**2.29**	3, 38, 39
EZH2	NM_004456	–	1.67	–	**2.30**	16, 20
FGFR2	NM_000141	–	**2.03**	1.66	**2.32**	
MX2	NM_002463	–	–	**2.75**	**2.32**	
EXO1[a]	NM_003686	1.91	1.84	–	**2.32**	
BMP6	NM_001718	–	–	–	**2.34**	2
WEE1	NM_003390	–	–	1.73	**2.35**	31
CSF2	NM_000758	–	1.79	–	**2.37**	2, 12
MDK[a]	NM_001012333	–	–	**2.23**	**2.40**	2, 8
ANXA3	NM_005139	–	1.51	–	**2.40**	1, 5
None	Z60461	–	–	–	**2.41**	
TTK	NM_003318	–	1.66	0.63	**2.43**	
ZFYVE20	NM_022340	1.65	–	–	**2.46**	
HMMR[a]	NM_012484	–	–	–	**2.49**	14
KRT18	NM_000224	–	–	–	**2.51**	
SERPINA1	NM_000295	–	**2.12**	–	**2.52**	1
IGFBP5	NM_000599	–	–	–	**2.52**	17, 38
ARC	NM_015193	–	–	–	**2.53**	
PRKY[a]	XM_497470	–	1.84	–	**2.54**	
NCAM1	NM_000615	1.67	**2.38**	–	**2.54**	
AP3B2	NM_004644	–	–	**2.26**	**2.56**	
TCEA2[a]	NM_003195	1.53	**2.53**	1.94	**2.57**	
ILF3[a]	NM_004516	–	–	–	**2.57**	

Table 1 (*continued*)

HUGO gene name	NCBI acc. no.	Fold induction/repression				Pathway ID
		GLI1 24 h	GLI1 72 h	GLI2 24 h	GLI2 72 h	
ADD3[a]	NM_001121	–	–	–	**2.58**	
MAD2L1[a]	NM_002358	1.58	1.90	–	**2.59**	26
RARRES3[a,b]	NM_004585	1.50	**2.04**	**2.37**	**2.63**	
BAP1	NM_004656	–	–	–	**2.64**	
GPR161	NM_007369	–	–	–	**2.68**	7
UBE2H	NM_003344	–	1.77	–	**2.69**	
AURKB	NM_004217	–	1.67	–	**2.71**	
BRCA1	NM_007294	–	1.87	–	**2.71**	13
SLC7A8	NM_012244	–	**2.46**	1.50	**2.73**	
PSAT1	NM_021154	–	1.76	1.76	**2.73**	
APC[a]	NM_000038	–	1.77	–	**2.74**	33
COL5A2[a]	NM_000393	–	–	–	**2.77**	25
LITAF[a]	NM_004862	–	1.58	**2.97**	**2.78**	
CKS1B[a,b]	NM_001826	–	**2.09**	–	**2.78**	9
CAMK1[a]	NM_003656	1.97	**3.07**	–	**2.78**	39
LRRN6A	NM_032808	–	**2.70**	–	**2.79**	
OAT[a]	NM_000274	–	–	1.92	**2.80**	
KIF11	NM_004523	–	**2.25**	–	**2.82**	
SEPT11[a]	NM_018243	–	–	**2.05**	**2.84**	
G1P2[a]	NM_005101	–	1.82	**2.16**	**2.84**	
PCNA[a]	NM_002592	**2.07**	**2.34**	–	**2.87**	8, 26, 31, 32
UBE2T	NM_014176	–	**2.25**	**0.48**	**2.89**	
LGALS1[a,b]	NM_002305	–	–	**2.12**	**2.93**	3, 13
LMNB1	NM_005573	–	1.86	–	**3.06**	
FZD7	NM_003507	–	1.73	–	**3.10**	12, 33
GPR160	NM_014373	–	–	1.64	**3.15**	
SERPINB2[a]	NM_002575	–	–	–	**3.15**	1, 40
C1orf183	NM_198926	–	1.74	–	**3.16**	
EP300	NM_001429	–	–	–	**3.16**	34
CDKN3[a]	NM_005192	–	**2.33**	0.58	**3.17**	
CTSL[a,b]	NM_001912	**2.35**	**7.52**	1.59	**3.30**	
IL1R2[a]	NM_004633	–	–	–	**3.30**	
FUS2	U73167	1.59	**2.71**	–	**3.44**	
FEN1[a]	NM_004111	1.66	1.69	**2.06**	**3.47**	
RGS19[a]	NM_005873	1.62	1.57	**2.08**	**3.54**	3, 38, 39
HTRA1[a]	NM_002775	**3.42**	**3.45**	**2.79**	**3.67**	17
GLI2	NM_005270	–	–	**2.57**	**3.80**	
TOP2A[a]	NM_001067	–	**2.00**	–	**3.83**	
CCNB1[b]	NM_031966	–	1.98	0.61	**3.88**	9, 31
CD40[a]	NM_001250	–	–	–	**3.90**	10, 11, 13, 40
KRT8	NM_002273	–	–	–	**3.98**	
CCNB2	NM_004701	–	**2.09**	–	**4.06**	9
CDC20[a]	NM_001255	–	**2.38**	–	**4.07**	8, 9, 12
KLK10[a,b]	NM_002776	–	–	**2.58**	**4.12**	
LARS2	NM_015340	–	–	–	**4.14**	18
ASPM[a]	NM_018136	–	**2.76**	–	**4.15**	
CDC45L[a,b]	NM_003504	–	**2.41**	–	**4.24**	31, 32
DHRS9[a]	NM_005771	**2.80**	**2.11**	**2.62**	**4.26**	
CDC2[a,b]	NM_001786	–	**2.91**	–	**4.37**	9
CENPF	NM_016343	–	1.97	–	**4.41**	26
CENPA[a]	NM_001809	–	**2.81**	–	**4.60**	16, 20, 24, 26, 29
PTCH[a,b]	NM_000264	**2.68**	**3.35**	**2.81**	**4.65**	8
ANLN[a]	NM_018685	–	**2.53**	–	**4.67**	
DLG7[a]	NM_014750	–	**3.39**	–	**4.88**	
UBE2C	NM_007019	–	1.77	–	**4.94**	9
TGM3[a]	NM_003245	**3.00**	**6.24**	**2.09**	**4.96**	
HRH1[a]	NM_000861	**2.39**	**3.66**	**3.98**	**5.00**	7, 10
PLCL1[a]	NM_006226	1.66	**2.70**	**2.09**	**5.19**	24
SIGLEC6	NM_001245	–	–	**4.50**	**5.34**	
EDN1[a]	NM_001955	1.95	**2.90**	**2.70**	**5.94**	

(continued on next page)

Table 1 (*continued*)

HUGO gene name	NCBI acc. no.	Fold induction/repression				Pathway ID
		GLI1 24 h	GLI1 72 h	GLI2 24 h	GLI2 72 h	
BCL2[a,b]	NM_000633	–	1.67	1.77	**6.41**	11, 13, 35
KIF23[a]	NM_138555	–	**2.94**	**0.49**	**6.46**	9
IL6[a]	NM_000600	–	**3.50**	–	**7.20**	2, 8, 11, 12, 38
SDC2	NM_002998	–	–	–	**7.45**	
FGF19[a]	NM_005117	1.97	**4.92**	1.93	**7.77**	
CPZ[a]	NM_001014447	–	**4.38**	–	**7.82**	
DOC1[a]	NM_014890	1.69	**4.41**	**2.09**	**8.49**	30
TNC[a,b]	NM_002160	**4.73**	**35.45**	**3.31**	**9.69**	25
FOXE1[a,b]	NM_004473	**2.62**	**4.97**	**5.55**	**10.38**	
KLK6[a,b]	NM_001012964	**2.88**	**6.79**	**2.70**	**10.45**	
CCL17[a]	NM_002987	1.66	**2.55**	**2.13**	**11.14**	2, 10, 19
FST[a,b]	NM_006350	1.69	**2.03**	**3.46**	**16.35**	34
BAMBI	NM_012342	–	–	**0.36**	–	
LOC440416	XM_498659	–	–	**0.38**	–	
IGF1R	NM_000875	–	–	**0.38**	–	
ACTR10	NM_018477	–	–	**0.39**	–	30
ANXA1	NM_000700	–	1.79	**0.40**	–	1, 5, 10, 12, 14, 24
SLC27A1	NM_198580	–	–	**0.40**	–	7
EIF2AK3[a]	NM_004836	0.62	–	**0.41**	–	18
GPR126	NM_020455	–	–	**0.41**	–	
PCBD1	NM_000281	–	–	**0.41**	–	
ST13	NM_003932	–	–	**0.42**	–	7
COX6C	NM_004374	–	–	**0.43**	–	41
PLA2G1B	NM_000928	–	–	**0.44**	–	
SMC6L1	NM_024624	–	–	**0.44**	–	
HLA-DQA2	NM_020056	–	0.59	**0.45**	–	
CHMP5	NM_016410	–	–	**0.45**	–	
CCNG2	NM_004354	–	–	**0.45**	–	9, 31
PRDX3	NM_006793	–	–	**0.45**	–	
BPGM	NM_001724	–	–	**0.46**	–	
DUSP14	NM_007026	–	–	**0.46**	–	40
RPLP2	NM_001004	–	–	**0.46**	–	7, 18
SUPT7L	NM_014860	–	–	**0.46**	–	
ERO1L	NM_014584	–	–	**0.47**	–	
ITGAE	NM_002208	–	–	**0.47**	–	
LAPTM5	NM_006762	–	–	**0.47**	–	
PDK1	NM_002610	–	–	**0.47**	–	41
XRCC1	NM_006297	–	–	**0.47**	–	
ZNF354B	NM_058230	–	–	**0.47**	–	
HSD11B2	NM_000196	0.65	0.63	**0.48**	–	15
AP1G1	NM_001030007	–	–	**0.48**	–	21
FBN1	NM_000138	–	–	**0.48**	–	25
PTD004	NM_013341	–	–	**0.48**	–	
SEPT3	NM_019106	–	–	**0.48**	–	9
SLMAP	NM_007159	–	–	**0.48**	–	
MERTK	NM_006343	0.59	**0.46**	**0.49**	–	12
EPX	NM_000502	–	–	**0.49**	–	
RGNEF	XM_371755	–	–	**0.49**	–	
GLRX2	NM_016066	–	–	**0.49**	–	13
KCMF1	NM_020122	–	–	**0.49**	–	
NDE1	NM_017668	–	–	**0.49**	–	
OGT	NM_181672	–	–	**0.49**	–	27
RIT1	NM_006912	–	–	**0.49**	–	
UBE2B	NM_003337	–	–	**0.49**	–	40
ZDHHC13	NM_019028	–	–	**0.49**	–	
DUSP2	NM_004418	–	–	**0.50**	–	
EBNA1BP2	NM_006824	–	–	**0.50**	–	
KIF9	NM_022342	–	–	**0.50**	–	
LIMK1	NM_002314	–	–	**0.50**	–	14, 36
NDUFB2	NM_004546	–	–	**0.50**	–	41

Table 1 (*continued*)

HUGO gene name	NCBI acc. no.	Fold induction/repression				Pathway ID
		GLI1 24 h	GLI1 72 h	GLI2 24 h	GLI2 72 h	
TCP1	NM_030752	–	–	**0.50**	–	7, 27
SLC28A1	NM_004213	**0.49**	**0.42**	1.91	–	
IQGAP1	NM_003870	–	–	**2.02**	–	1, 3, 30, 36
SFRP1[a]	NM_003012	**2.17**	**2.33**	**2.04**	–	
CD24	NM_013230	–	–	**2.07**	–	11
DAZAP2	NM_014764	–	0.63	**2.09**	–	40
CREG	NM_003851	–	–	**2.10**	–	8
COX6B	NM_001863	–	–	**2.15**	–	41
PLA2G4C	NM_003706	–	–	**2.17**	–	5, 10, 22, 27
EEF1G	NM_001404	0.52	**0.44**	**2.21**	–	18, 37
DHRSX	NM_145177	–	–	**2.33**	–	
SLC7A5	NM_003486	–	–	**2.36**	–	
HMGA2	NM_001015886	–	–	**2.49**	–	16, 20, 26, 29
KRTHB3	NM_002282	**2.17**	0.62	**3.23**	–	
KRT6L[a]	NM_175834	–	–	**3.99**	–	
KRT2A	NM_000423	–	**0.45**	**6.17**	–	
ASS	NM_000050	0.61	**0.28**	–	–	
IGFBP3[a]	NM_000598	–	**0.38**	–	–	17, 38
MMP12[a]	NM_002426	–	**0.42**	–	–	4, 14, 25
CALR	NM_004343	0.64	**0.43**	–	–	39
RPL13A	NM_012423	–	**0.43**	–	–	7
ZNF496	NM_032752	0.54	**0.45**	–	–	
FAM14A	NM_032036	–	**0.49**	–	–	
UACA	NM_001008224	–	**2.04**	–	–	
ECHDC1[a]	NM_018479	–	**2.11**	–	–	7
GAS1	NM_002048	–	**2.12**	–	–	
MGC27165	AF067420	–	**2.12**	–	–	
LCE2B[a,b]	NM_014357	1.81	**2.13**	–	–	
MOSPD3	NM_023948	1.70	**2.14**	–	–	
INHBB[a]	NM_002193	1.65	**2.27**	–	–	2
BDNF[a]	NM_001709	1.81	**3.30**	–	–	
C3AR1	NM_004054	**0.45**	–	–	–	7, 10, 14, 19
GPX7	NM_015696	**2.02**	–	–	–	
SMC2L1	NM_006444	**2.08**	–	–	–	16
VGLL4	NM_014667	**2.20**	–	–	–	

Genes differentially expressed are sorted by fold induction/repression values of the GLI2ΔN 72-h time point. Gene names represent approved gene symbols according to the HUGO Gene Nomenclature Committee (http://www.gene.ucl.ac.uk/nomenclature). Genes without a HUGO gene name are written in italic. Genes named "None" represent Incyte EST sequences, which do not show any significant match with annotated nucleotide sequences in the GenBank/GenPept databases. Pathway ID numbers refer to Fig. 4. White background, induced gene; gray background, repressed gene; light face, gene significant at fold-change ≥1.5; bold face, gene significant at fold-change ≥2.0; –, no significant value.

[a] Resequenced EST clone.

[b] Verified by QRT-PCR.

and differentiation-opposing effects of the two oncogenic transcription factors. The identity of differentially expressed genes reflects the activity of signaling pathways previously implicated in keratinocyte and hair follicle differentiation. The data support the view that GLI transcription factors have overlapping yet distinct activities. There are clear quantitative differences in the effects of the two transcription factors on a small number of positively regulated genes such as *TNC*, *FST*, and *BCL2* (Figs. 5B and 5C). The activated form of GLI2, GLI2ΔN, effects massive target gene repression, whereas only weak repression is seen with GLI1 expression. Phosphorylation of GLI2 by PKA without evidence for proteolytic processing favors the interpretation that no Ci/GLI3-like product is responsible for the repression of most GLI2 target genes. These results suggest that GLI2ΔN may specifically activate the transcription of a repressor, which would then act

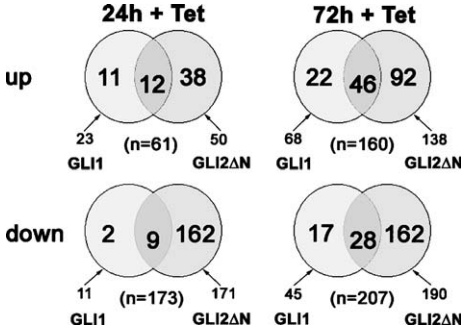

Fig. 2. Changes in gene expression after induction of GLI1 or GLI2ΔN by tetracycline in HaCaT keratinocytes. Venn diagram of the array data comparing the inducing and repressing activities of GLI1 and GLI2ΔN. Genes changing ≥2.0-fold in response to GLI1 or expression after 24 and 72 h were included. The total number of genes induced or repressed by each transcription factor is indicated below.

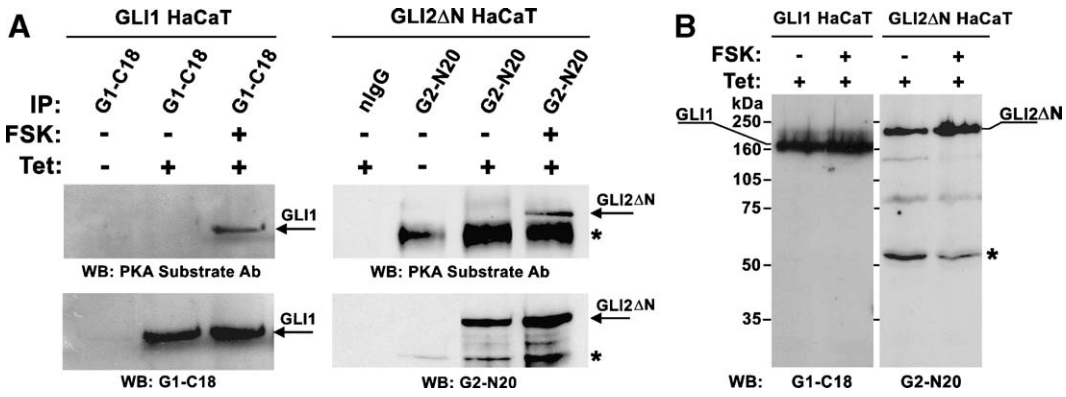

Fig. 3. GLI1 and GLI2ΔN are phosphorylated in the presence of forskolin, but not proteolytically processed. (A) Immunoprecipitation (IP) showing phosphorylation of GLI1 and GLI2ΔN by protein kinase A (PKA) upon forskolin (FSK) treatment. GLI1 and GLI2ΔN were immunoprecipitated from FSK-treated cells expressing GLI1 (GLI1 HaCaT) or GLI2ΔN (GLI2ΔN HaCaT) using GLI-specific antibodies (G1-C18, G2-N20) or normal goat IgG. Phosphorylated GLIs were visualized with a primary antibody recognizing phosphorylated PKA sites (PKA substrate Ab) (top) and anti GLI antibodies (bottom). (B) No lower molecular bands of GLI1 or GLI2ΔN protein were observed in GLI1 HaCaT or GLI2ΔN HaCaT cells upon FSK treatment. Total lysates of tetracycline-induced cells grown for 48 h in the presence of FSK and controls were analyzed by Western blot using specific antibodies recognizing GLI1 and GLI2. Nonspecific signals are marked by asterisks.

on target genes. Alternatively or additionally, other modifications of GLI2 or interactions with other GLI molecules [22] or unrelated further factors may result in gain of repressive activity. A more comprehensive picture of the mechanism of the overlaps and specificities of the GLI proteins will emerge from the clarification of these issues.

Material and methods

Cell cultures

HaCaT cells were cultured in Dulbecco's modified Eagle medium (pH 7.2, high glucose; Invitrogen Life Technologies) supplemented with 10% fetal calf serum (Invitrogen Life Technologies), 100 μg/ml streptomycin, and 62.5 μg/ml

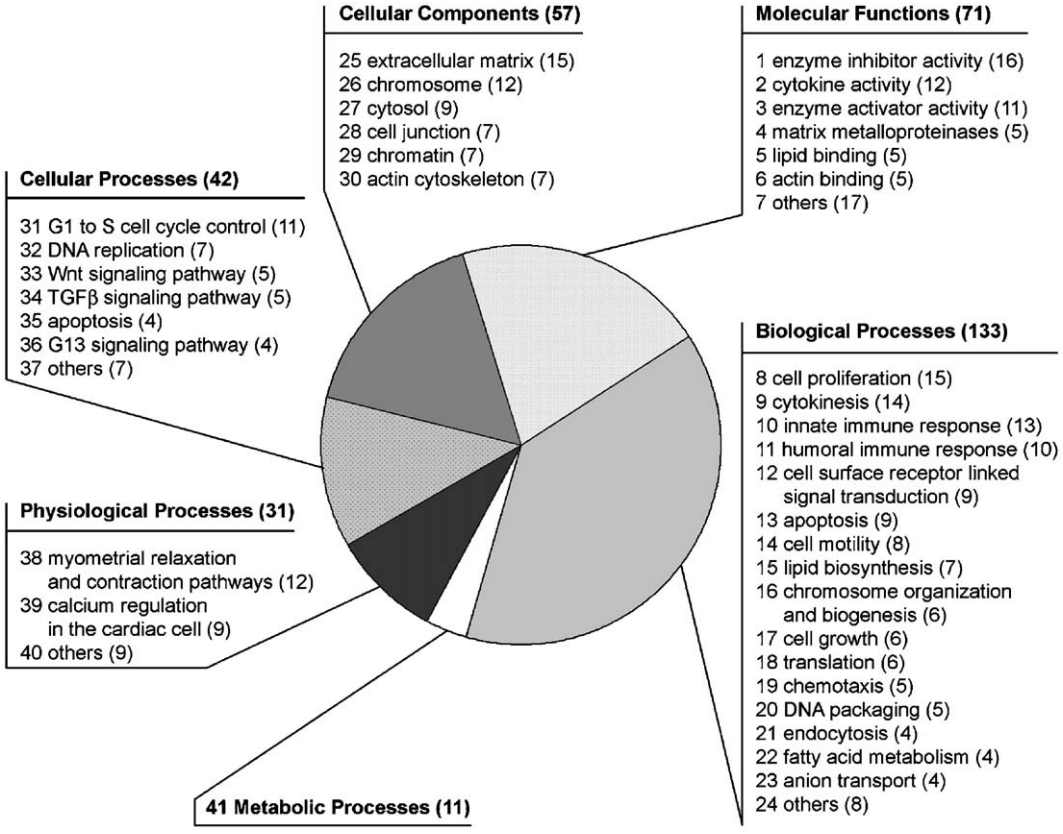

Fig. 4. Functional clustering of up- and downregulated genes. Clustering of array data was carried out using the Pathway explorer software (https://www.pathwayexplorer.genome.tugraz.at/). Grouping of genes refers to the GenMapp pathway or functional group classification. 196 of 456 differentially expressed genes were mapped to 41 pathways or functional groups (see Table 1); for the remaining genes no match was found. Most of the 196 genes gave matches in more than one pathway (total of 345 hits). Groups with fewer than 4 members are pooled in "others." The number of hits found in each group is shown in parentheses. Numbers in front of each gene group denote the pathway ID as shown in Table 1.

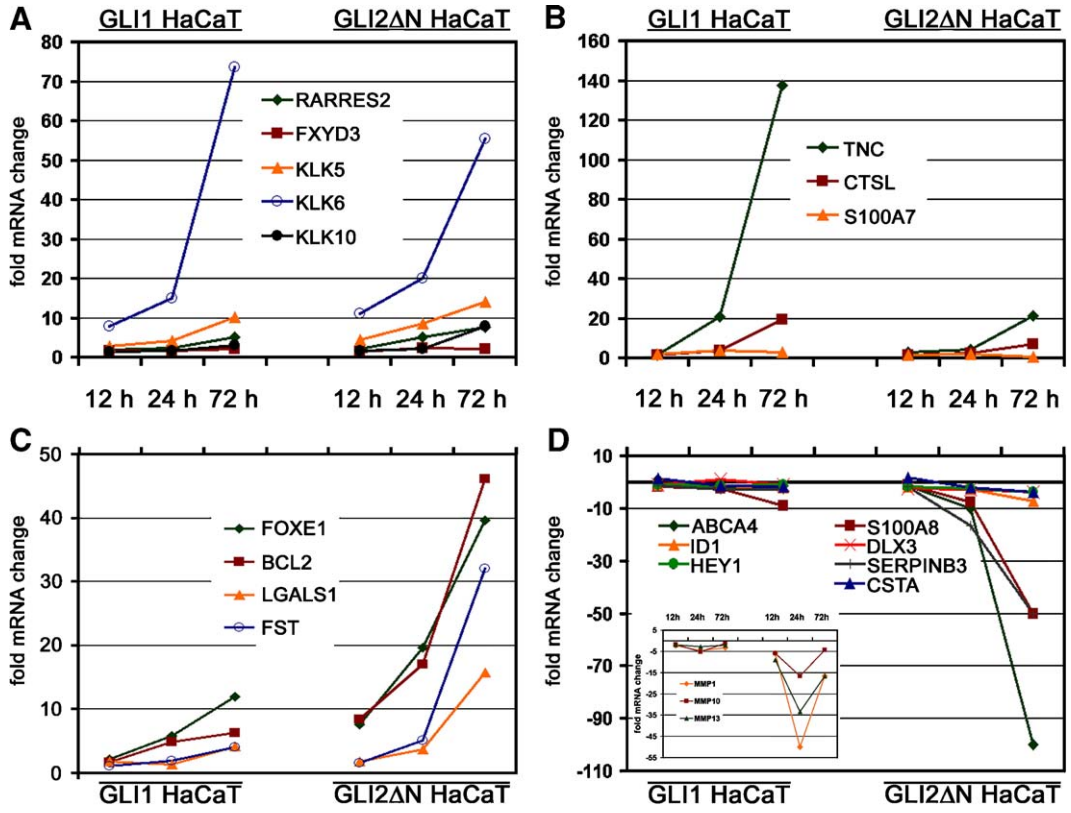

Fig. 5. Expression patterns of representative GLI1 and GLI2ΔN target genes. Induction of target genes was measured by QRT-PCR. Fold change refers to the ratios of RNA from cells induced with tetracycline for the times indicated to uninduced cells. (A) Genes with similar expression patterns in response to GLI1 and GLI2ΔN overexpression. (B) Genes preferentially induced by GLI1. (C) Genes preferentially induced by GLI2ΔN. (D) Genes preferentially repressed by GLI2ΔN.

penicillin (Sigma–Aldrich) at 37°C, 5% CO_2. For PKA activation, forskolin (in EtOH) (Sigma–Aldrich) was added to a final concentration of 10 μM. Controls were treated with EtOH only.

Double stable inducible HaCaT lines expressing either human GLI1 (GLI1 HaCaT) or GLI2ΔN tagged with a 6×HIS epitope (GLI2ΔN HaCaT) [43] were grown in the presence of 25 μg/ml zeocin (Invitrogen Life Technology) and 8 μg/ml Blasticidin-S (ICN-Biomedica). Transgene expression was induced by adding 1 μg/ml tetracycline (Tet) (Invitrogen Life Technologies) to the medium.

Preparation of ^{33}P-labeled cDNA

Total RNA was extracted with TRI reagent (Molecular Research Center) according to the manufacturer's instructions followed by LiCl precipitation. To eliminate differences between clonal cell lines, RNA from four independently isolated lines expressing either GLI1 or GLI2ΔN was pooled for cDNA array analysis. cDNA labeling was carried out as described previously [75]. In brief, 15 μg pooled total RNA was reverse transcribed with Superscript II (Invitrogen Life Technologies) in the presence of 70 μCi [α-^{33}P]dCTP (3000 Ci/mmol;

Table 2
Roles of GLI1 and GLI2ΔN in proliferation and differentiation

Gene name	GLI1 HaCaT			GLI2ΔN HaCaT		
	12 h+Tet fl/R (±SD)	24 h+Tet fl/R (±SD)	72 h+Tet fl/R (±SD)	12 h+Tet fl/R (±SD)	24 h+Tet fl/R (±SD)	72 h+Tet fl/R (±SD)
CCNA2	0.97 (±0.044)	0.86 (±0.101)	7.49 (±0.127)	0.98 (±0.039)	1.46 (±0.166)	5.63 (±0.437)
CDC2	1.10 (±0.133)	1.07 (±0.151)	6.07 (±0.515)	1.06 (±0.039)	1.18 (±0.137)	5.59 (±0.271)
CDC45L	1.17 (±0.277)	2.64 (±0.068)	13.39 (±0.808)	0.85 (±0.093)	2.39 (±0.398)	14.39 (±0.747)
E2F1	1.17 (±0.071)	3.45 (±0.179)	4.96 (±0.069)	0.64 (±0.013)	3.99 (±0.097)	9.85 (±0.102)
CCNB1	1.27 (±0.313)	1.24 (±0.215)	4.84 (±0.625)	1.03 (±0.046)	0.85 (±0.103)	4.84 (±0.351)
CKS1B	0.93 (±0.030)	1.35 (±0.082)	3.54 (±0.878)	1.04 (±0.054)	1.26 (±0.087)	4.96 (±0.394)
CCNE	0.86 (±0.085)	1.80 (±0.069)	1.49 (±0.288)	0.82 (±0.010)	1.74 (±0.024)	4.11 (±0.107)
CDKN1A	0.99 (±0.072	0.52 (±0.028)	0.71 (±0.039	0.56 (±0.010)	0.32 (±0.020	0.38 (±0.054
KRT1	1.27 (±0.048)	0.81 (±0.050)	0.67 (±0.286)	1.00 (±0.323)	0.15 (±0.006)	0.04 (±0.019)
KRT10	0.83 (±0.079)	0.55 (±0.030)	0.45 (±0.088)	0.98 (±0.267)	0.09 (±0.001)	0.01 (±0.005)
IVL	0.80 (±0.041)	0.56 (±0.018)	0.32 (±0.025)	1.21 (±0.623)	0.25 (±0.041)	0.04 (±0.002)
PI3	0.83 (±0.041)	0.37 (±0.013)	0.25 (±0.044)	1.25 (±0.222)	0.20 (±0.024)	0.10 (±0.027)
SPRR2A	0.82 (±0.206)	0.49 (±0.068)	0.34 (±0.177)	1.15 (±0.837)	0.18 (±0.005)	0.05 (±0.003)

Ratios and SD were calculated from the average of four real-time RT-PCR measurements.

Amersham Biosciences). Labeled cDNA was purified with GFX DNA purification columns (Amersham Biosciences) and equal counts of labeled cDNA were added to each hybridization.

High-density DNA filter array production and hybridization

The Human Drug Discovery clone set (10,000 sequence-verified ESTs) and a selection of 2000 sequence-verified EST clones from the human UniGem version 2.0 library were obtained from Incyte Genomics. Both sets were amplified by PCR, spotted, and hybridized separately with labeled cDNA. PCR amplification, array production, and hybridization were done as described previously [60,75]. Arrays were exposed for 4 days and scanned with a BAS-1800II (Fuji) phosphorimager. Array images were analyzed using the AIDA Metrix suite (Raytest). Data from two independent hybridizations were collected at each time point. Data were normalized by total signal intensity and the statistical significance was analyzed using the SAM software package [48]. Only genes showing at least a 2-fold change in expression were called significant. For genes reaching this threshold at one time point, further points were analyzed also at 1.5-fold change.

The data discussed in this publication have been deposited in the NCBI Gene Expression Omnibus (GEO; http://www.ncbi.nlm.nih.gov/geo/) and are accessible through GEO Series Accession No. GSE 1434.

QRT-PCR analysis

RNA prepared as described above was further purified with the High Pure RNA isolation kit (Roche) to remove any genomic contamination. cDNA was synthesized from 4 μg purified total RNA with Superscript II (Invitrogen) using oligo(dT) primers, according to the manufacturer's instructions. QRT-PCR analysis was performed on a Rotorgene 2000 (Corbett Research) using iQTM SYBR Green Supermix (Bio-Rad). Primer sequences not published previously [43,60] are shown in Table 3 (supplementary material). Large ribosomal protein P0 (RPLP0) was used as a reference in all QRT-PCR analyses [76].

Immunoprecipitation and Western blot analysis

GLI1 HaCaT and GLI2ΔN HaCaT cells were lysed 24 h after Tet induction in RIPA buffer (150 mM NaCl, 0.1% SDS, 10 mM Tris–HCl, pH 7.4, 1% Triton X-100, 1% sodium deoxycholate, 1 mM PMSF, 1 mM protease inhibitor mix (Sigma–Aldrich)) at 4°C. Lysates were cleared by centrifugation (15 min, 13,000 rpm, 4°C) and incubated overnight with the appropriate antibody at 4°C. After incubation with protein G–Sepharose (Amersham Biosciences) for 2 h at 4°C, the Sepharose was washed four times with RIPA buffer and proteins were eluted in hot lysis buffer (125 mM Tris (pH 6.8), 5% glycerol, 2% SDS, 1% β-mercaptoethanol, 0.006% bromophenol blue) and resolved by SDS–PAGE. SDS–PAGE and Western blotting were performed according to standard protocols. Primary and secondary antibodies used were goat polyclonal anti-GLI2 (GLI2 N20; Santa Cruz), goat polyclonal anti-GLI1 (GLI1 C18; Santa Cruz), rabbit anti-phospho-(Ser/Thr) PKA substrate antibody (Cell Signaling Technologies), anti-rabbit IgG–HRP (Santa Cruz), and rabbit anti-goat IgG–HRP (Chemicon).

Luciferase reporter assay

HaCaT cells were grown in 12-well plates to 80% confluence and transfected in triplicate with GLI1, GLI2ΔN [43], GLI2 [34], and *Renilla* luciferase (pRL-SV40 (Promega)) expression plasmids and pGL3 luciferase reporter plasmids as indicated in Fig. 1B. Cells were harvested 48 h after transfection and luciferase activity was measured with a Lucy II luminometer (Anthos) using the dual-luciferase reporter assay system (Promega) according to the manufacturer's instructions. Data were normalized for *Renilla* luciferase activity.

Acknowledgments

We thank S. Siller for excellent technical assistance and Dr. Maximilian Muenke for providing the full-length GLI2 expression construct. This work was supported by FWF Project P14227, GEN-AU Project "Ultra-sensitive Proteomics and Genomics," the University of Salzburg program "Biosciences and Health," and a predoctoral fellowship of the Austrian Academy of Science to V.S.

Appendix A. Supplementary data

Supplementary data associated with this article can be found in the online version at doi:10.1016/j.ygeno.2005.12.003.

References

[1] P.W. Ingham, A.P. McMahon, Hedgehog signaling in animal development: paradigms and principles, Genes Dev. 15 (2001) 3059–3087.
[2] J.E. Hooper, M.P. Scott, Communicating with Hedgehogs, Nat. Rev. Mol. Cell Biol. 6 (2005) 306–317.
[3] A. Ruiz i Altaba, P. Sanchez, N. Dahmane, Gli and hedgehog in cancer: tumours, embryos and stem cells, Nat. Rev. Cancer 2 (2002) 361–372.
[4] P. Sanchez, V. Clement, A. Ruiz i Altaba, Therapeutic targeting of the Hedgehog–GLI pathway in prostate cancer, Cancer Res. 65 (2005) 2990–2992.
[5] M. Pasca di Magliano, M. Hebrok, Hedgehog signalling in cancer formation and maintenance, Nat. Rev. Cancer 3 (2003) 903–911.
[6] D.N. Watkins, D.M. Berman, S.B. Baylin, Hedgehog signaling: progenitor phenotype in small-cell lung cancer, Cell Cycle 2 (2003) 196–198.
[7] B. Stecca, A. Ruiz i Altaba, Brain as a paradigm of organ growth: Hedgehog–Gli signaling in neural stem cells and brain tumors, J. Neurobiol. 64 (2005) 476–490.
[8] E. Nieuwenhuis, C.C. Hui, Hedgehog signaling and congenital malformations, Clin. Genet. 67 (2005) 193–208.
[9] H. Hahn, et al., Mutations of the human homolog of Drosophila patched in the nevoid basal cell carcinoma syndrome, Cell 85 (1996) 841–851.
[10] R.L. Johnson, et al., Human homolog of patched, a candidate gene for the basal cell nevus syndrome, Science 272 (1996) 1668–1671.
[11] M.R. Gailani, et al., The role of the human homologue of Drosophila patched in sporadic basal cell carcinomas, Nat. Genet. 14 (1996) 78–81.
[12] J. Xie, et al., Activating Smoothened mutations in sporadic basal-cell carcinoma, Nature 391 (1998) 90–92.
[13] J. Reifenberger, et al., Missense mutations in SMOH in sporadic basal cell carcinomas of the skin and primitive neuroectodermal tumors of the central nervous system, Cancer Res. 58 (1998) 1798–1803.
[14] H. Fan, A.E. Oro, M.P. Scott, P.A. Khavari, Induction of basal cell carcinoma features in transgenic human skin expressing Sonic Hedgehog, Nat. Med. 3 (1997) 788–792.
[15] A.E. Oro, et al., Basal cell carcinomas in mice overexpressing sonic hedgehog, Science 276 (1997) 817–821.
[16] N. Dahmane, J. Lee, P. Robins, P. Heller, A. Ruiz i Altaba, Activation of the transcription factor Gli1 and the Sonic hedgehog signalling pathway in skin tumours, Nature 389 (1997) 876–881.
[17] M. Grachtchouk, et al., Basal cell carcinomas in mice overexpressing Gli2 in skin, Nat. Genet. 24 (2000) 216–217.
[18] M. Nilsson, et al., Induction of basal cell carcinomas and trichoepitheliomas in mice overexpressing GLI-1, Proc. Natl. Acad. Sci. U. S. A. 97 (2000) 3438–3443.
[19] H. Sheng, et al., Dissecting the oncogenic potential of Gli2: deletion of an NH(2)-terminal fragment alters skin tumor phenotype, Cancer Res. 62 (2002) 5308–5316.
[20] A.E. Oro, K. Higgins, Hair cycle regulation of Hedgehog signal reception, Dev. Biol. 255 (2003) 238–248.
[21] H.L. Park, et al., Mouse Gli1 mutants are viable but have defects in SHH signaling in combination with a Gli2 mutation, Development 127 (2000) 1593–1605.
[22] V. Nguyen, A.L. Chokas, B. Stecca, A.R. Altaba, Cooperative requirement of the Gli proteins in neurogenesis, Development 132 (2005) 3267–3279.

[23] A.R. Altaba, Gli proteins encode context-dependent positive and negative functions: implications for development and disease, Development 126 (1999) 3205–3216.
[24] L. Buttitta, R. Mo, C.C. Hui, C.M. Fan, Interplays of Gli2 and Gli3 and their requirement in mediating Shh-dependent sclerotome induction, Development 130 (2003) 6233–6243.
[25] J. Motoyama, et al., Essential function of Gli2 and Gli3 in the formation of lung, trachea and oesophagus, Nat. Genet. 20 (1998) 54–57.
[26] R. Mo, et al., Specific and redundant functions of Gli2 and Gli3 zinc finger genes in skeletal patterning and development, Development 124 (1997) 113–123.
[27] C.B. Bai, W. Auerbach, J.S. Lee, D. Stephen, A.L. Joyner, Gli2, but not Gli1, is required for initial Shh signaling and ectopic activation of the Shh pathway, Development 129 (2002) 4753–4761.
[28] C.B. Bai, A.L. Joyner, Gli1 can rescue the in vivo function of Gli2, Development 128 (2001) 5161–5172.
[29] M. Hynes, et al., Control of cell pattern in the neural tube by the zinc finger transcription factor and oncogene Gli-1, Neuron 19 (1997) 15–26.
[30] H. Sasaki, Y. Nishizaki, C. Hui, M. Nakafuku, H. Kondoh, Regulation of Gli2 and Gli3 activities by an amino-terminal repression domain: implication of Gli2 and Gli3 as primary mediators of Shh signaling, Development 126 (1999) 3915–3924.
[31] A. Ruiz i Altaba, Combinatorial Gli gene function in floor plate and neuronal inductions by Sonic hedgehog, Development 125 (1998) 2203–2212.
[32] P. Aza-Blanc, H.Y. Lin, A. Ruiz i Altaba, T.B. Kornberg, Expression of the vertebrate Gli proteins in Drosophila reveals a distribution of activator and repressor activities, Development 127 (2000) 4293–4301.
[33] C. von Mering, K. Basler, Distinct and regulated activities of human Gli proteins in Drosophila, Curr. Biol. 9 (1999) 1319–1322.
[34] E. Roessler, et al., A previously unidentified amino-terminal domain regulates transcriptional activity of wild-type and disease-associated human GLI2, Hum. Mol. Genet. 14 (2005) 2181–2188.
[35] Q. Ding, et al., Diminished Sonic hedgehog signaling and lack of floor plate differentiation in Gli2 mutant mice, Development 125 (1998) 2533–2543.
[36] P. Mill, et al., Sonic hedgehog-dependent activation of Gli2 is essential for embryonic hair follicle development, Genes Dev. 17 (2003) 282–294.
[37] M.E. Hutchin, et al., Sustained Hedgehog signaling is required for basal cell carcinoma proliferation and survival: conditional skin tumorigenesis recapitulates the hair growth cycle, Genes Dev. 19 (2005) 214–223.
[38] P. Sanchez, et al., Inhibition of prostate cancer proliferation by interference with SONIC HEDGEHOG–GLI1 signaling, Proc. Natl. Acad. Sci. U. S. A. 101 (2004) 12561–12566.
[39] L. Ghali, S.T. Wong, J. Green, N. Tidman, A.G. Quinn, Gli1 protein is expressed in basal cell carcinomas, outer root sheath keratinocytes and a subpopulation of mesenchymal cells in normal human skin, J. Invest. Dermatol. 113 (1999) 595–599.
[40] S.S. Karhadkar, et al., Hedgehog signalling in prostate regeneration, neoplasia and metastasis, Nature 431 (2004) 707–712.
[41] H. Kimura, D. Stephen, A. Joyner, T. Curran, Gli1 is important for medulloblastoma formation in Ptc1(+/−) mice, Oncogene (2005).
[42] P. Boukamp, et al., Normal keratinization in a spontaneously immortalized aneuploid human keratinocyte cell line, J. Cell Biol. 106 (1988) 761–771.
[43] G. Regl, et al., Human GLI2 and GLI1 are part of a positive feedback mechanism in basal cell carcinoma, Oncogene 21 (2002) 5529–5539.
[44] A. Tanimura, S. Dan, M. Yoshida, Cloning of novel isoforms of the human Gli2 oncogene and their activities to enhance tax-dependent transcription of the human T-cell leukemia virus type 1 genome, J. Virol. 72 (1998) 3958–3964.
[45] M. Agren, P. Kogerman, M.I. Kleman, M. Wessling, R. Toftgard, Expression of the PTCH1 tumor suppressor gene is regulated by alternative promoters and a single functional Gli-binding site, Gene 330 (2004) 101–114.
[46] M.S. Ikram, et al., GLI2 is expressed in normal human epidermis and BCC and induces GLI1 expression by binding to its promoter, J. Invest. Dermatol. 122 (2004) 1503–1509.
[47] P. Dai, et al., Sonic Hedgehog-induced activation of the Gli1 promoter is mediated by GLI3, J. Biol. Chem. 274 (1999) 8143–8152.
[48] V.G. Tusher, R. Tibshirani, G. Chu, Significance analysis of microarrays applied to the ionizing radiation response, Proc. Natl. Acad. Sci. U. S. A. 98 (2001) 5116–5121.
[49] G. Regl, et al., Activation of the BCL2 promoter in response to Hedgehog/GLI signal transduction is predominantly mediated by GLI2, Cancer Res. 64 (2004) 7724–7731.
[50] K.W. Kinzler, B. Vogelstein, The GLI gene encodes a nuclear protein which binds specific sequences in the human genome, Mol. Cell Biol. 10 (1990) 634–642.
[51] B. Wang, J.F. Fallon, P.A. Beachy, Hedgehog-regulated processing of Gli3 produces an anterior/posterior repressor gradient in the developing vertebrate limb, Cell 100 (2000) 423–434.
[52] M. Persson, et al., Dorsal–ventral patterning of the spinal cord requires Gli3 transcriptional repressor activity, Genes Dev. 16 (2002) 2865–2878.
[53] C.B. Bai, D. Stephen, A.L. Joyner, All mouse ventral spinal cord patterning by hedgehog is Gli dependent and involves an activator function of Gli3, Dev. Cell 6 (2004) 103–115.
[54] S.H. Shin, P. Kogerman, E. Lindstrom, R. Toftgard, L.G. Biesecker, GLI3 mutations in human disorders mimic Drosophila cubitus interruptus protein functions and localization, Proc. Natl. Acad. Sci. U. S. A. 96 (1999) 2880–2884.
[55] Y. Litingtung, C. Chiang, Specification of ventral neuron types is mediated by an antagonistic interaction between Shh and Gli3, Nat. Neurosci. 3 (2000) 979–985.
[56] M.A. Price, D. Kalderon, Proteolysis of cubitus interruptus in Drosophila requires phosphorylation by protein kinase A, Development 126 (1999) 4331–4339.
[57] Y. Chen, N. Gallaher, R.H. Goodman, S.M. Smolik, Protein kinase A directly regulates the activity and proteolysis of cubitus interruptus, Proc. Natl. Acad. Sci. U. S. A. 95 (1998) 2349–2354.
[58] B. Wang, J.F. Fallon, P.A. Beachy, Hedgehog-regulated processing of Gli3 produces an anterior/posterior repressor gradient in the developing vertebrate limb, Cell 100 (2000) 423–434.
[59] B. Mlecnik, et al., PathwayExplorer: web service for visualizing high-throughput expression data on biological pathways, Nucleic Acids Res. 33 (2005) W633–W637.
[60] G. Regl, et al., The zinc-finger transcription factor GLI2 antagonizes contact inhibition and differentiation of human epidermal cells, Oncogene 23 (2004) 1263–1274.
[61] E. Hernando, et al., Rb inactivation promotes genomic instability by uncoupling cell cycle progression from mitotic control, Nature 430 (2004) 797–802.
[62] T. Eichberger, et al., FOXE1, a new transcriptional target of GLI2 is expressed in human epidermis and basal cell carcinoma, J. Invest. Dermatol. 122 (2004) 1180–1187.
[63] W. Potts, et al., Cathepsin L-deficient mice exhibit abnormal skin and bone development and show increased resistance to osteoporosis following ovariectomy, Int. J. Exp. Pathol. 85 (2004) 85–96.
[64] F. Benavides, et al., Impaired hair follicle morphogenesis and cycling with abnormal epidermal differentiation in nackt mice, a cathepsin L-deficient mutation, Am. J. Pathol. 161 (2002) 693–703.
[65] W. Roth, et al., Cathepsin L deficiency as molecular defect of furless: hyperproliferation of keratinocytes and perturbation of hair follicle cycling, FASEB J. 14 (2000) 2075–2086.
[66] E. Frohlich, M. Mohrle, C. Klessen, Cathepsins in basal cell carcinomas: activity, immunoreactivity and mRNA staining of cathepsins B, D, H and L, Arch. Dermatol. Res. 295 (2004) 411–421.
[67] V.A. Botchkarev, et al., Modulation of BMP signaling by noggin is required for induction of the secondary (nontylotrich) hair follicles, J. Invest. Dermatol. 118 (2002) 3–10.
[68] V.A. Botchkarev, A.A. Sharov, BMP signaling in the control of skin development and hair follicle growth, Differentiation 72 (2004) 512–526.
[69] A.G. Li, M.I. Koster, X.J. Wang, Roles of TGFbeta signaling in epidermal/appendage development, Cytokine Growth Factor Rev. 14 (2003) 99–111.
[70] A. De Luca, et al., Pattern of expression of HtrA1 during mouse development, J. Histochem. Cytochem. 52 (2004) 1609–1617.

[71] M. Nakamura, et al., Control of pelage hair follicle development and cycling by complex interactions between follistatin and activin, FASEB J. 17 (2003) 497–499.
[72] F. Vinals, et al., BMP-2 decreases Mash1 stability by increasing Id1 expression, EMBO J. 23 (2004) 3527–3537.
[73] A. Hollnagel, V. Oehlmann, J. Heymer, U. Ruther, A. Nordheim, Id genes are direct targets of bone morphogenetic protein induction in embryonic stem cells, J. Biol. Chem. 274 (1999) 19838–19845.
[74] T. Katagiri, et al., Identification of a BMP-responsive element in Id1, the gene for inhibition of myogenesis, Genes Cells 7 (2002) 949–960.
[75] F. Aberger, et al., Analysis of gene expression using high-density and IFN-gamma-specific low-density cDNA arrays, Genomics 77 (2001) 50–57.
[76] K.J. Martin, et al., High-sensitivity array analysis of gene expression for the early detection of disseminated breast tumor cells in peripheral blood, Proc. Natl. Acad. Sci. U. S. A. 98 (2001) 2646–2651.